IEEE Photonics Journal
An IEEE Photonics Society Publication

Simple Design of a Wideband and Wide-Angle Insensitive Metamaterial Absorber Using Lumped Resistors for X- and Ku-Bands

Volume 13, Number 3, June 2021

Thi Kim Thu Nguyen
Thanh Nghia Cao
Ngoc Hieu Nguyen
Le Dac Tuyen
Xuan Khuyen Bui
Chi Lam Truong
Dinh Lam Vu
Thi Quynh Hoa Nguyen

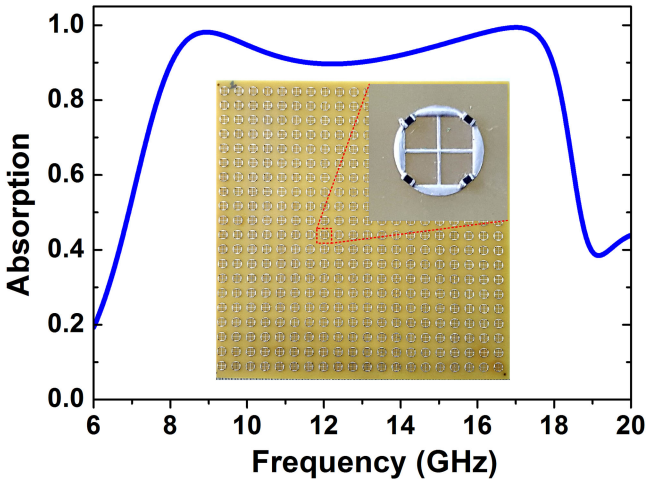

DOI: 10.1109/JPHOT.2021.3085320

IEEE photonics SOCIETY
IEEE

Simple Design of a Wideband and Wide-Angle Insensitive Metamaterial Absorber Using Lumped Resistors for X- and Ku-Bands

Thi Kim Thu Nguyen,[1,2] Thanh Nghia Cao,[1] Ngoc Hieu Nguyen,[1] Le Dac Tuyen,[3] Xuan Khuyen Bui,[4] Chi Lam Truong,[5] Dinh Lam Vu,[2] and Thi Quynh Hoa Nguyen [1]

[1] School of Engineering and Technology, Vinh University, Vinh 460000, Vietnam
[2] Graduate University of Science and Technology, Vietnam Academy of Science and Technology, Hanoi 100000, Vietnam
[3] Department of Physics, Hanoi University of Mining and Geology Hanoi 100000, Vietnam
[4] Institute of Materials Science, Vietnam Academy of Science and Technology, Hanoi 100000, Vietnam
[5] NTT Hi-Tech Institute, Nguyen Tat Thanh University, Ho Chi Minh City 700000, Vietnam

DOI:10.1109/JPHOT.2021.3085320

Manuscript received March 8, 2021; revised May 26, 2021; accepted May 26, 2021. Date of publication June 1, 2021; date of current version June 21, 2021. This work was supported by the Ministry of Education and Training, Vietnam under Grant B2021-TDV-05. Corresponding author: Thi Quynh Hoa Nguyen (e-mail: ntqhoa@vinhuni.edu.vn).

Abstract: We report a wideband and polarization-/wide-angle insensitive metamaterial absorber based on a symmetry structure associated with surface mount resistors. The proposed structure consists of a periodic array of a top metal symmetry resonator loading with four lumped resistors and a continuous metal ground plane separated by a dielectric substrate of FR-4. A prototype of the proposed absorber is fabricated and measured, confirming a good agreement between the measurement and simulation results. The proposed absorber shows polarization-insensitive behavior and the absorption response in a frequency range from 8-18 GHz covering the entire X- and Ku- bands with an absorptivity above 80% for a wide incident angle up to 40° for both transverse electric and transverse magnetic polarizations. Compared with the reported broadband absorbers using lumped resistors, our proposed absorber exhibits excellent characteristics in terms of compact and simple structure, high relative absorption bandwidth, and polarization and wide-incident insensitivity. Therefore, this design shows promising potential for both X- and Ku-band applications.

Index Terms: Holography, image analysis.

I. Introduction

Metamaterials have attracted enormous attention with various potential applications in perfect lens [1]–[3], holograms [4], [5], invisibility cloaking [6], [7], polarization converter [8], [9] and perfect absorber [10], [11] due to their exotic properties. Among them, metamaterial absorber (MA) is one of the fastest-growing field for solar cells [12], [13], thermal emitter [14]–[16], antenna design [17], [18], and imaging and sensing [11], [19]–[21] applications. Until now, the MAs have been realized to absorb the electromagnetic (EM) waves from microwave, infrared to visible region. However, the

bandwidth of MA is narrow because of its natural resonance. Therefore, many approaches have been proposed to extend the bandwidth of MAs such as using planar arrangement of various sizes of resonators in unit-cell [22]–[25], vertical stacking of metal-dielectric multilayer [26]–[30], and planar fractal structure [31]–[34]. Despite broadening of absorption bandwidth, some problems have been made by these methods. For example, the fabrication process of vertical stacking is very complicated, while the planar arrangement method possesses functional limitations such as polarization-dependency and sensitivity to oblique incidence [35]. Meanwhile, the design of broadband MA based on a planar fractal structure is not efficient in microwave range [34]. Recently, the symmetry structures based on lumped elements can be considered as an emerging and promising alternative for designing the broadband absorber with large enough bandwidth, high efficiency, and polarization insensitivity [36]–[42]. Li *et al.* proposed the thin and polarization-insensitive wideband MA formed by loading eight lumped resistors into double octagonal rings, which showed a 9.25 GHz-wide absorption from 7.93 to 17.18 GHz with absorptivity larger than 90%, however, the angular stability is still small below 20^o[36]. Chen *et al.* designed a microwave metamaterial absorber using lumped resistors and metallic via holes which exhibited the absorption bandwidth covering the entire X- and Ku-bands [41]. Furthermore, Bagmanci *et al.* demonstrated the polarization-independent broadband MA structure created by loaded with the lumped resistors and via connection lines into split-ring resonators. The simulation results indicate that the proposed broadband absorber achieved a perfect absorption from 4 GHz to 16 GHz [42]. The combination of metallic shorting pins and lumped resistors can be good candidates for broadening the absorption bandwidth and keeping the wide angular stability [41], [42], but this method still needs a complex manufacturing process, thus resisting their practical applications. Therefore, the design of the MA based on lumped resistors is facing significant challenges to achieve a simple structure, wide bandwidth, and good absorption performance such as polarization and wide incident angle insensitivity, simultaneously.

Herein, we propose a simple design of an ultra-broadband and wide-angle and polarization insensitive MA using symmetry structure loading by lumped resistors operating in X- and Ku-bands. The proposed MA is composed of a periodic array of a metal symmetry-shaped resonator loaded by four lumped resistors, and a dielectric substrate of FR4 backed with a bottom metal continuous ground plane. The absorption performance of the proposed MA is numerically and experimentally investigated. The designed MA achieves an ultra-broadband absorption response with the absorptivity above 90% in the frequency range from 8 to 18 GHz covering the entire X- and Ku-bands. Moreover, the absorption efficiency is retained higher than 80% in the whole band with a wide incident angle for both transverse electric (TE) and transverse magnetic (TM) polarizations. Therefore, this designed structure can be used for X-and Ku-band applications.

II. Structure Design and Method

Fig. 1 shows a schematic of the proposed MA. The unit cell of the proposed MA consists of a metallic resonator loaded with four lumped resistors and a dielectric substrate backed by a metal continuous ground plane, as presented in Fig. 1(a). The dielectric substrate is made by FR-4 with the thickness (h) of 2.5 mm. The FR-4 substrate has a relative dielectric constant of 4.3 and a loss tangent of 0.025. The top and the bottom layers are made of copper with an electric conductivity of 5.96×10^7 S/m and a thickness of 0.035 mm. This study aims to design a broadband MA operating in the range of 8-18 GHz, which covers the entire X- and Ku-bands. To aid the design structure, the simulation method was carried out to optimize the geometrical parameters of the proposed MA.

In particular, we use the commercial computer simulation technology (CST) Microwave Studio 2013 software with a frequency-domain solver to optimize the designed parameters as well as analyze the performance of the proposed MA. In the simulation setup, the periodic boundary conditions are fixed to unit cell for the x and y directions, and the open boundary condition is set in the z-direction. The incident wave (k) is polarized along z direction. The tetrahedral mesh is applied in the model with an accuracy of 10^{-4}.

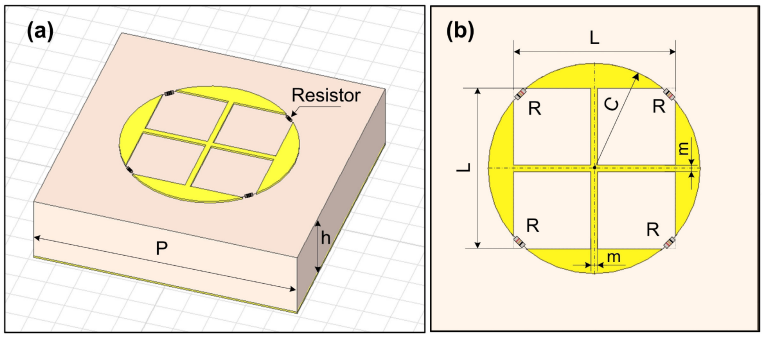

Fig. 1. Schematic of the proposed MA: (a) 3D-view and (b) top view of a unit cell.

TABLE I
Optimized Parameters of the Proposed MA

Parameter	P	h	L	C	m	R
Value	9.7 (mm)	2.5 (mm)	4.8 (mm)	3.15 (mm)	0.2 (mm)	240 (Ω)

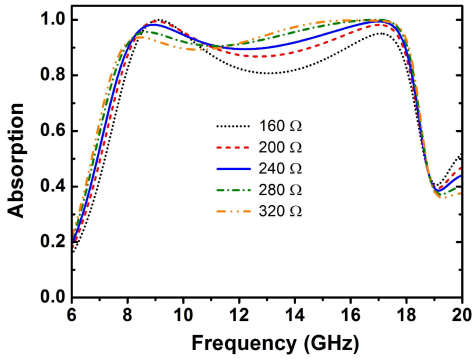

Fig. 2. Absorption spectra of the proposed MA with various values of lumped resistor.

The absorption of the MA can be calculated as equation (1).

$$A(\omega) = 1 - R(\omega) - T(\omega) = 1 - \left|S_{11}(\omega)\right|^2 - \left|S_{21}(\omega)\right|^2 \tag{1}$$

where, $R(\omega) = S_{11}(\omega)$ and $T(\omega) = S_{21}(\omega)$ represent reflection and transmission, respectively. Due to the entire ground plane covers by copper, the transmission becomes zero, thus absorption is simply given by equation (2).

$$A(\omega) = 1 - \left|S_{11}(\omega)\right|^2 \tag{2}$$

The MA design aims to work in the frequency range of 8–18 GHz covering the entire X- and Ku-bands with an absorption efficiency higher than 90%. To achieve this design goal, we have optimized structural parameters by analyzing the effect of geometrical parameters of *h* in the range of 1.9-3.1 mm, *P* in the range of 8.7-10.7 mm, *C* in the range of 2.75-3.35 mm, *L* in the range of 2.3–2.6 mm, *m* in the range of 0.1-0.5 mm, and *R* in range of 160-320 Ω on the absorption spectra of the proposed MA. Based on the evaluation of simulation results in such a way that absorption spectrum is the widest and its efficiency is the highest, the design parameter optimization of the proposed MA structure is gathered as shown in Table I. With changing the value of lumped resistors in the range from 160 - 320 Ω, the absorption bandwidth is almost unchanged, as shown in Fig. 2. This is due to the resonances is created when the imaginary part of the input admittance

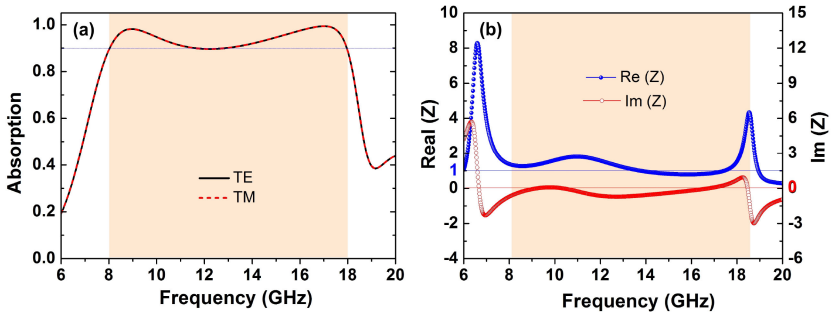

Fig. 3. (a) Absorption spectra and (b) the normalized impedance of the proposed MA under normal incidence.

equals zero [43], [44]. The imaginary part of the input admittance depends only on the inductor and capacitor parameters determined by the shape of metallic resonator of the unit cell but not on lumped resistor (R). However, the R parameter determines the input impedance of MA, thus leading to the change in the absorptivity of the proposed MA as seen in Fig. 2. The absorptivity is above 90% in the desired frequency band ranging from 8 - 18 GHz when R varies from 240 to 280 Ω. Therefore, in this design, the R is chosen at 240 Ω to obtain strong resonant peaks.

III. Results and Discussion

Fig. 3(a) shows the absorption spectra of the proposed MA for both TE and TM polarizations. The absorption spectra of the proposed MA for TE and TM polarizations are superimposed to each other. It possesses the absorption response with absorptivity above 90% in a wide frequency band from 8 - 18 GHz covering the entire X- and Ku-bands. Furthermore, two distinct absorption peaks are found at 8.9 GHz and 17.1 GHz, with corresponding absorptivities of 98.2% and 99.4%, respectively. The relative bandwidth is used to evaluate the absorption performance of the MA, which is calculated as equation (3), where f_U and f_L are the highest and lowest frequency of absorption band with absorptivity higher than 90%. It proves the relative bandwidth (RBW) of the proposed MA can reach to 76.92%, indicating that the designed MA achieves the ultra-broadband absorption properties.

$$RBW = 2 \times \frac{f_U - f_L}{f_U + f_L} \tag{3}$$

The absorption mechanism of the proposed MA can be explained by the impedance matching between the MA structure and the free space. The normalized impedance of the MA is given by equation (4) [45], [46].

$$Z = \sqrt{\frac{(1 + S_{11})^2 - S_{21}^2}{(1 - S_{11})^2 - S_{21}^2}} = \frac{1 + S_{11}}{1 - S_{11}}. \tag{4}$$

Due to its impedance matching, a smaller amount of power is reflected from the structure thus maximum absorptivity occurs at the desired frequency band. Fig. 3(b) shows the normalized impedance of the proposed MA. It is seen that real and imaginary part are nearly unity and zero over a wide frequency range from 8 to 18 GHz which confirms the presence of broadband absorption.

To further investigate the physical mechanism, we have simulated the electric field and surface current distributions of the proposed MA at the resonant frequencies of 8.9 GHz and 17.1 GHz in the XOY plane, as presented in Fig. 4. As seen in Figs. 4(a) and (d), the electric field is concentrated at a particular part of MA corresponding to a specific frequency. At the lower resonant frequency

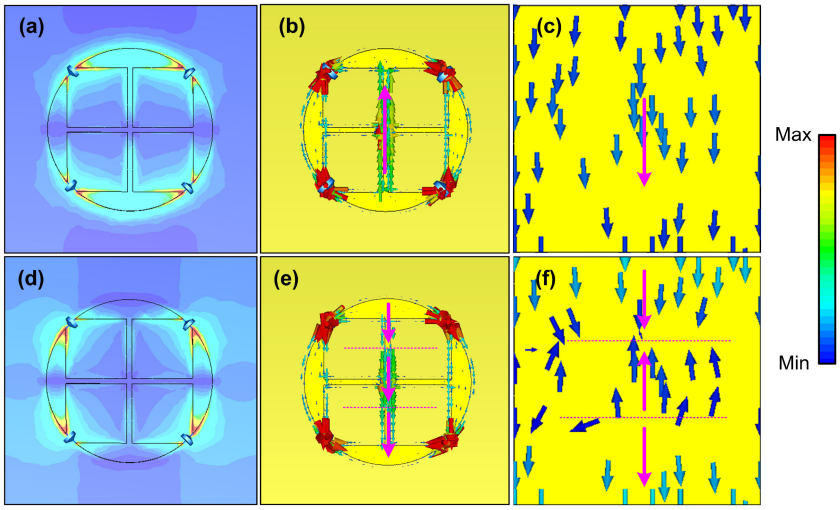

Fig. 4. (a),(d) the electric field distribution and surface current distributions on (b),(e) the top layer and (c),(f) the bottom layer of the proposed absorber at the resonant frequencies of 8.9 GHz and 17.1 GHz, respectively.

of 8.9 GHz, the electric field harvests at the gaps and the vertical shape of the metallic resonator. Meanwhile, at the resonant frequency of 17.1 GHz, the electric field accumulates at the gaps and the horizontal shape of the metallic resonator. The surface current distributions on the top and bottom metallic layer of the proposed MA at 8.9 GHz and 17.1 GHz are presented in Figs. 4(b),(c) and (e),(f), respectively. It is clear from Figs. 4(b) and (c), at the lower frequencies of 8.9 GHz, the top surface current is anti-parallel with the bottom surface current, indicating that the magnetic resonance is contributed to the resonant frequency. At the higher resonant frequency of 17.1 GHz, the bottom surface current is divided to three regions, where the currents on adjacent regions are anti-parallel, as shown in Fig. 4(f). Meanwhile, the top surface current is kept in the same direction in the three regions as seen in Fig. 4(e). This interesting effect is caused by the same order of the periodicity and the operational wavelength at 17.1 GHz. Therefore, the periodic metallic patterns of proposed MA can be regarded as a two-dimensional metallic grating, which creates the guided-mode resonances (GMRs) [47]–[51]. It was reported that the magnetic resonance excited in MA structure that obtained the wide-angle insensitivity for both TE and TM polarizations [52], [53]. It is due to the forming of the induced magnetic field inside the MA structure that can efficient trap the incident magnetic field for wide-incident angle. Furthermore, the efficient and wide-angle broadband absorption response is attributed to the existing of the GMR resonances in the meta-surface structure [54]. Therefore, wide-angle insensitive wideband absorption response in the proposed design loaded lumped resistors is due to the synergy of magnetic and GMR resonances.

For practical applications, the design MA can maintain the broadband absorption response with a wide incident angle that is a main important factor because the electromagnetic (EM) wave is obliquely incident onto the surface. Thus, the simulated dependence of the absorptivity on the frequency and the incident angles in the range of 0-50° for both TE and TM polarizations is implemented, as depicted in Fig. 5. It can be seen that for both polarizations, the absorptivity of the proposed MA decreases with increasing the incident angle. However, the proposed absorber can maintain the high absorption intensity above 70 % with increasing the incident angle up to 50° for both TE and TM polarizations. Moreover, the absorptivity can keep as high as 80% in the whole operating frequency range from 8 GHz to 12 GHz, when incident angle changes from 0° to 35° for TE polarization and 0° to 40° for TE polarization. It indicates that the proposed MA has a good broadband absorption performance for a wide incident angle.

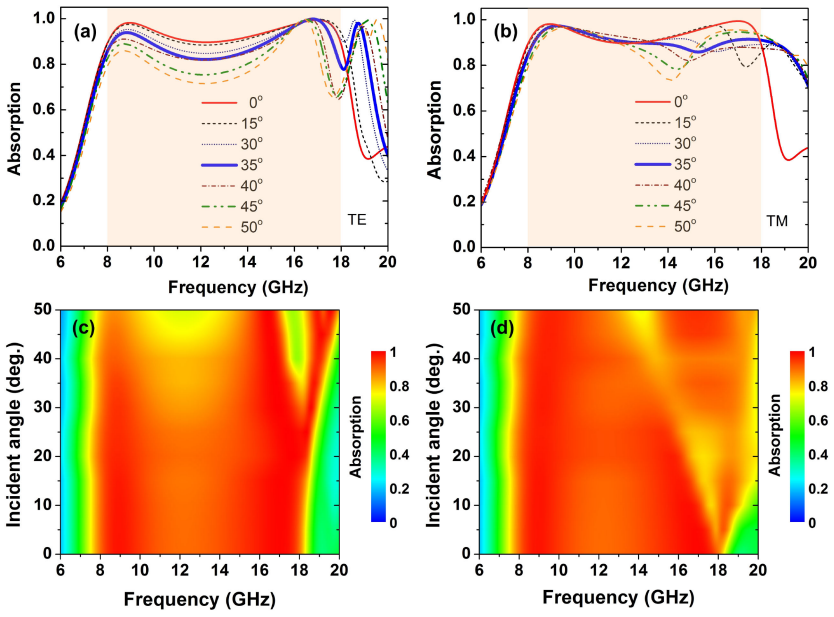

Fig. 5. Absorption spectra and the corresponding absorption maps of the proposed MA with different incident angles for (a),(c) TE and (b),(d) TM polarizations, respectively.

We also investigate the effect of the polarization angle on the performance of the proposed MA for both TE and TM polarizations. It can be seen in Fig. 6, for both polarizations, the absorptivity is not changed in the whole operation frequency band (8-18 GHz) with varying of the polarization angle from 0 to 90°. It proves that the proposed MA is polarization insensitivity due to its symmetry structure.

To verify the performance of the designed MA, device fabrication was using the conventional photolithography process. The structural parameters of the fabrication sample are fixed the same as the simulated model. The material used in the device fabrication is the copper coated FR-4 substrate on both sides with a copper thickness of 0.035 mm, FR-4 substrate thickness of 2.5 mm, and a relative dielectric constant of 4.3. The surface mount resistors with size 0402 and resistance of 240 Ω with 1% tolerance are chosen as lumped resistors. The fabricated sample image is illustrated in Fig. 7, which contains 20 × 20 unit cells and 1600 resistors and has an oversize of 194 mm × 194 mm. To analyze the absorption performance of fabricated MA, the reflection coefficients as a function of frequency were measured by the Rohde and Schwarz ZNB20 vector network analyzer together with two identical linearly polarized standard-gain horn antennas as transmitter and receiver. The measurement data are collected in the range of 6-18 GHz. Fig. 8 shows the measured absorption spectra of fabricated MA with various oblique angles of 10°, 30° and 40° for TE and TM polarizations. It can be observed that the experimental results are in good agreement with the simulation results. The measured absorptivity keeps higher than 0.8 in the range of 8-18 GHz with incident angle up to 40° for both TE and TM polarizations. It confirms that the designed MA is a wide incident angle insensitivity.

Finally, we have compared the performance of the proposed MA with other recently reported broadband MAs designed based on lumped resistors. Table II shows the MA properties in terms of operating frequency, the periodicity of unit-cell and thickness with respect to the lowest absorption frequency, relative bandwidth, and unit-cell characteristics including the number of layers and lumped resistors. It can be seen from Tab. II, the proposed design has a simple structure with the smallest thickness and moderate periodicity and excellent performance characterized by the highest relative bandwidth per layer as well as per lumped resistor, simultaneously.

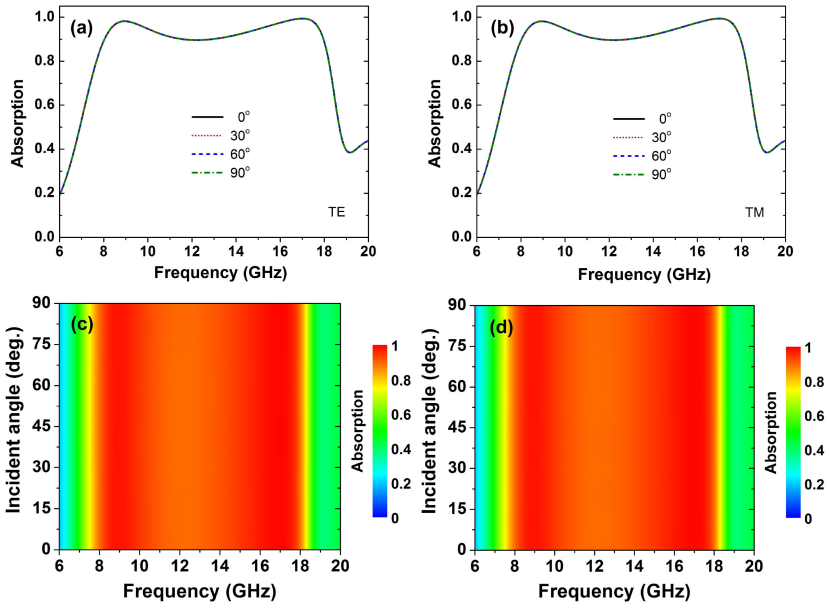

Fig. 6. Absorption spectra and the corresphonding absorption maps of the proposed MA with different polarization angles under normal incidence for (a),(c) TE and (b),(d) TM polarizations, respectively.

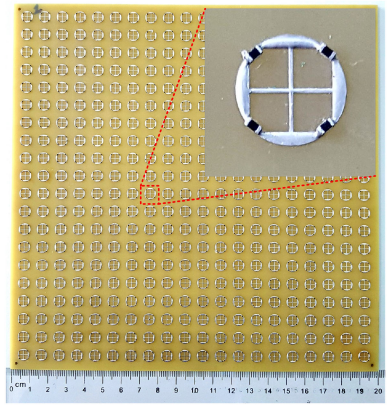

Fig. 7. The image of the fabricated sample and its enlarged view.

TABLE II

Comparison the Performance of the Proposed MA With Other Broadband MAs

Ref.	Working frequency (GHz)	Periodicity of unit-cell (mm)	Thickness (mm)	RBW (%)	Unit-cell characteristics	
					No. layers	No. resistors
[55]	7.2 - 12.5	12.8×12.8 (0.31λ_L)	5.2 (0.125λ_L)	53.81	3	6
[56]	5.2 - 18	13×13 (0.23λ_L)	4.8 (0.083λ_L)	110.35	3	12
[57]	7.6 - 18.3	10×10 (0.25λ_L)	3.25 (0.082λ_L)	82.63	2	4
[58]	3.9 - 10.5	12.5×12.5 (0.16λ_L)	7.57 (0.098λ_L)	91.67	2	4
[59]	8.2 - 13.4	15.5×15.5 (0.42λ_L)	3.0 (0.082λ_L)	48.15	1	8
[60]	8 - 18	13×13 (0.36λ_L)	3.175 (0.085λ_L)	76.92	1	8
[61]	7 - 12.8	14×14 (0.33λ_L)	3.4(0.079λ_L)	58.59	1	4
This work	8 - 18	9.7×9.7 (0.26λ_L)	2.5 (0.067λ_L)	76.92	1	4

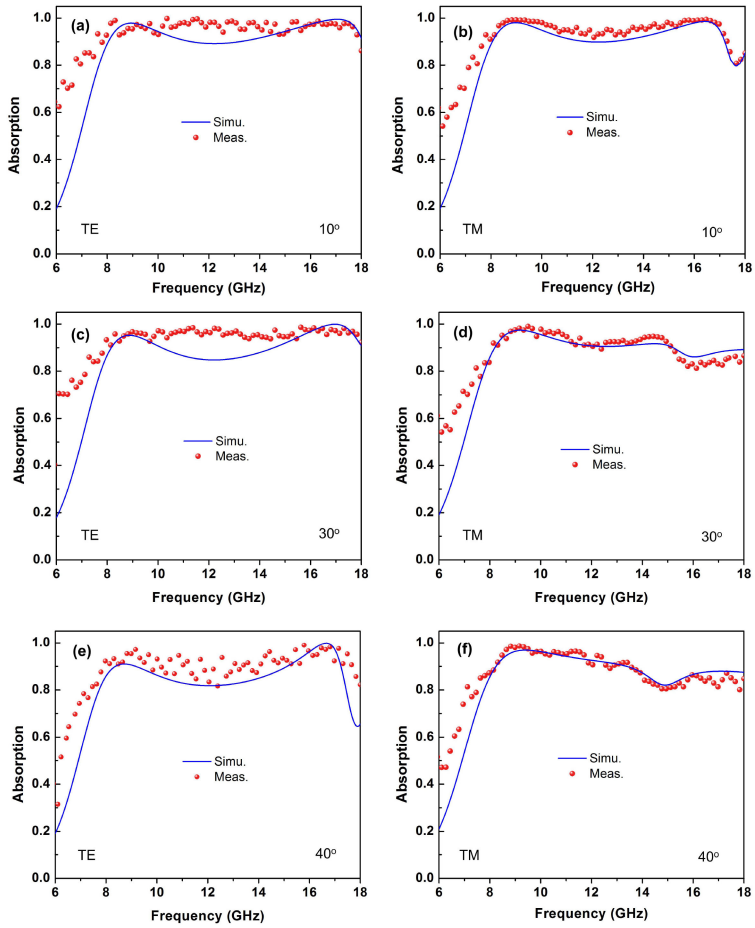

Fig. 8. The measured absorption spectra of the fabricated MA under various incident angles of 10°, 30°, and 40° for (a),(c),(e) TE and (b),(d),(f) TM polarizations, respectively.

IV. Conclusion

We have proposed a wideband and polarization-wide-angle insensitive MA based on symmetry structure with surface mount resistors operating in the X- and Ku-bands. The proposed structure is composed of a periodic array of a top metal symmetry resonator loading with four lumped resistors, a dielectric substrate of FR-4 backed a continuous metal ground plane. The absorption performance of the proposed absorber is analyzed by both simulation and experiment. The experimental result shows that the proposed MA can maintain the absorptivity above 80% in a frequency range from 8-18 GHz for a wide incident angle up to 40° for both TE and TM polarizations. Moreover, the proposed MA is insensitive to polarization due to its symmetry structure. The physical absorption mechanism has been explained by a thorough analysis of the impedance and surface current distribution. Besides, compared with other absorbers based on lumped resistors, our design has a simple and compact structure, and excellent performance such as high relative absorption bandwidth, polarization, and wide-incident insensitivity. Therefore, these suggest that this design is a promising candidate for X- and Ku-band applications.

References

[1] J. B. Pendry, "Negative refraction makes a perfect lens," *Phys. Rev. Lett.*, vol. 85, pp. 3966–3969, 2000.

[2] A. Arbabi, Y. Horie, A. J. Ball, M. Bagheri, and A. Faraon, "Subwavelength-thick lenses with high numerical apertures and large efficiency based on high-contrast transmitarrays," *Nature Commun*, vol. 6, no. 1, 2015, Art. no. 7069.
[3] M. Khorasaninejad and F. Capasso, "Metalenses: Versatile multifunctional photonic components," *Science*, vol. 358, no. 6367, 2017, Art. no. eaam8100.
[4] D. Wen *et al.*, "Helicity multiplexed broadband metasurface holograms," *Nature Commun*, vol. 6, no. 1, 2015, Art. no. 8241.
[5] E. Almeida, O. Bitton, and Y. Prior, "Nonlinear metamaterials for holography," *Nature Commun.*, vol. 7, 2016, Art. no. 12533.
[6] J. B. Pendry, D. Schurig, and D. R. Smith, "Controlling electromagnetic fields," *Science*, vol. 312, pp. 1780–1782, 2016.
[7] H. Chen, C. T. Chan, and P. Sheng, "Transformation optics and metamaterials," *Nature Mater.*, vol. 9, pp. 387–396, 2010.
[8] T. K. T. Nguyen *et al.*, "Simple design of efficient broadband multifunctional polarization converter for x-band applications," *Sci. Rep.*, vol. 11, 2011, Art. no. 2032.
[9] T. Q. H. Nguyen *et al.*, "Simple design of a wideband and wide-angle reflective linear polarization converter based on crescent-shaped metamaterial for ku-band applications," *Opt. Commun.*, vol. 456, 2021, Art. no. 126773.
[10] N. I. Landy, S. Sajuyigbe, J. J. Mock, D. R. Smith, and W. J. Padilla, "Perfect metamaterial absorber," *Phys. Rev. Lett.*, vol. 100, 2008, Art. no. 207402.
[11] N. Liu, M. Mesch, T. Weiss, M. Hentschel, and H. Giessen, "Infrared perfect absorber and its application as plasmonic sensor," *Nano Lett.*, vol. 10, no. 7, pp. 2342–2348, 2010.
[12] Y. Wang, T. Sun, T. Paudel, Y. Zhang, Z. Ren, and K. Kempa, "Metamaterial-plasmonic absorber structure for high efficiency amorphous silicon solar cells," *Nano Lett.*, vol. 12, no. 1, pp. 440–445, 2012.
[13] P. Rufangura and C. Sabah, "Dual-band perfect metamaterial absorber for solar cell applications," *Vacuum*, vol. 120, pp. 68–74, 2015.
[14] X. Liu, T. Tyler, T. Starr, A. F. Starr, N. M. Jokerst, and W. J. Padilla, "Taming the blackbody with infrared metamaterials as selective thermal emitters," *Phys. Rev. Lett.*, vol. 107, no. 4, 2011, Art. no. 045901.
[15] L. Peng, D. Liu, H. Cheng, S. Zhou, and M. Zu, "A multilayer film based selective thermal emitter for infrared stealth technology," *Adv. Opt. Mater.*, vol. 6, no. 23, 2018, Art. no. 1801006.
[16] A. Kong, B. Cai, P. Shi, and X.-C. Yuan, "Ultra-broadband all-dielectric metamaterial thermal emitter for passive radiative cooling," *Opt. Exp.*, vol. 27, no. 21, pp. 30102–30115, 2019.
[17] X. Liu, J. Gao, L. Xu, X. Cao, Y. Zhao, and S. Li, "A coding diffuse metasurface for RCS reduction," *IEEE Antennas Wireless Propag. Lett.*, vol. 16, pp. 724–727, 2016.
[18] J. Ren, S. Gong, and W. Jiang, "Low-RCS monopolar patch antenna based on a dual-ring metamaterial absorber," *IEEE Antennas Wireless Propag. Lett.* vol. 17, no. 1, pp. 102–105, 2018.
[19] X. Hu *et al.*, "Metamaterial absorber integrated microfluidic terahertz sensors," *Laser Photon. Rev.*, vol. 10, pp. 962–969, 2016.
[20] Y. Wen *et al.*, "Photomechanical meta-molecule array for real-time terahertz imaging," *Microsyst. Nanoeng.*, vol. 3, 2017, Art. no. 17071.
[21] J. Grant, M. Kenney, Y. D. Shah, I. Escorcia-Carranza, and D. R. S. Cumming, "CMOS compatible metamaterial absorbers for hyperspectral medium wave infrared imaging and sensing applications," *Opt. Exp.* vol. 26, no. 8, pp. 10408–10420, 2018.
[22] D. T. Viet *et al.*, "Perfect absorber metamaterials: Peak, multi-peak and broadband absorption," *Opt. Commun.*, vol. 322, no. 1, pp. 209–213, 2014.
[23] W. Ma, Y. Wen, and X. Yu, "Broadband metamaterial absorber at mid-infrared using multiplexed cross resonators," *Opt. Exp.*, vol. 21, no. 25, 2013, Art. no. 30724.
[24] H. Wang and L. Wang, "Perfect selective metamaterial solar absorbers," *Opt. Exp.*, vol. 21, no. 106, 2013, Art. no. A1078.
[25] G. Shen, M. Zhang, Y. Ji, W. Huang, H. Yu, and J. Shi, "Broadband terahertz metamaterial absorber based on simple multi-ring structures," *AIP Adv.*, vol. 8, 2018, Art. no. 075206.
[26] F. Ding, Y. Cui, X. Ge, Y. Jin, and S. He, "Ultra-broadband microwave metamaterial absorber," *Appl. Phys. Lett.*, vol. 100, 2012, Art. no. 103506.
[27] Y. Cui *et al.*, "Ultrabroadband light absorption by a sawtooth anisotropic metamaterial slab," *Nano Lett.*, vol. 12, pp. 1343–1347, 2012.
[28] N. T. Q. Hoa, P. D. Tung, and P. H. Lam, "Wide-angle and polarization-independent broadband microwave metamaterial absorber," *Microw. Opt. Technol. Lett.*, vol. 59, no. 5, pp. 1157–1161, 2017.
[29] N. T. Q. Hoa, P. H. Lam, P. D. Tung, T. S. Tuan, and H. Nguyen, "Numerical study of a wide-angle and polarization-insensitive ultrabroadband metamaterial absorber in visible and near-infrared region," *IEEE Photon. J.*, vol. 11, no. 1, Feb. 2019, Art. no. 4600208.
[30] T. S. Tuan and N. T. Q. Hoa, "Numerical study of an efficient broadband metamaterial absorber in visible light region," *IEEE Photon. J.*, vol. 11, no. 3, Jun. 2019, Art no. 4600810.
[31] M. Kenney, J. Grant, and D. R. S. Cumming, "Alignment-insensitive bilayer THz metasurface absorbers exceeding 100% bandwidth," *Opt. Exp.*, vol. 27, no. 15, pp. 20886–20900, 2019.
[32] M. Kenney, J. Grant, Y. D. Shah, I. Escorcia-Carranza, M. Humphreys, and D. R. Cumming, "Octave-spanning broadband absorption of terahertz light using metasurface fractal-cross absorbers," *ACS Photon.*, vol. 4, pp. 2604–12, 2017.
[33] P. C. Wu, N. Papasimakis, and D. P. Tsai, "Self-affine graphene metasurfaces for tunable broadband absorption," *Phys. Rev. Appl.*, vol. 6, 2016, Art. no. 044019.
[34] S. Fan and Y. Song, "Bandwidth-enhanced polarization-insensitive metamaterial absorber based on fractal structures," *J. App. Phys., vol.* 123, no. 8, 2018, Art. no. 085110.
[35] P. Yu *et al.*, "Broadband metamaterial absorbers," *Adv. Optical. Mater.*, vol. 17, 2019, Art. no. 1800995.

[36] S. Li, J. Gao, X. Cao, W. Li, Z. Zhang, and D. Zhang, "Wideband, thin, and polarization-insensitive perfect absorber based the double octagonal rings metamaterials and lumped resistances," *J. App. Phys.*, vol. 116, 2014, Art. no. 043710.
[37] T. Q. H. Nguyen, T. K. T. Nguyen, T. N. Cao, H. Nguyen, and L. G. Bach, "Numerical study of a broadband metamaterial absorber using a single split circle ring and lumped resistors for x-band applications," *AIP Adv.*, vol. 10, 2020, Art. no. 035326.
[38] Y. Z. Cheng, Y. Wang, Y. Niea, R. Z. Gong, X. Xiong, and X. Wang, "Design, fabrication and measurement of a broadband polarization-insensitive metamaterial absorber based on lumped elements," *J. Appl. Phys.*, vol. 111, 2012, Art. no. 044902.
[39] D. Lee, H. Jeong, and S. Lim, "Electronically switchable broadband metamaterial absorber," *Sci. Rep.*, vol. 7, 2017, Art. no. 4891.
[40] Y. J. Kim, Y. J. Yoo, J. S. Hwang, and Y. P. Lee, "Ultra-broadband microwave metamaterial absorber based on resistive sheets," *J. Opt.*, vol. 19, 2017, Art. no. 015103.
[41] K. Chen, X. Luo, G. Ding, J. Zhao, Y. Feng, and T. Jiang, "Broadband microwave metamaterial absorber with lumped resistor loading," *EPJ Appl. Metamaterials*, vol. 6, pp. 1–7, 2019.
[42] M. Bagmanci, O. Akgol, M. Ozakturk, M. Karaaslan, E. Unal, and M. Bakir, "Polarization independent broadband metamaterial absorber for microwave applications," *Int. J. RF Microw. Comput. Aided Eng.*, vol. 29, no. 1, 2018, Art. no. e21630.
[43] D. Kundu, A. Mohan, and A. Chakrabarty, "Single-layer wide-band microwave absorber using array of crossed dipoles," *IEEE Antennas Wireless Propag. Lett.*, vol. 15, pp. 1589–1592, 2016.
[44] Z. Yao, S. Xiao, Z. Jiang, L. Yan, and B.-Z. Wang, "On the design of ultrawideband circuit analog absorber based on quasi-single-layer FSS," *IEEE Antennas Wireless Propag. Lett.*, vol. 19, no. 4, pp. 591–595, Apr. 2020.
[45] S. Bhattacharyya and K. V. Srivastava, "Triple band polarization-independent ultra-thin metamaterial absorber using electric field-driven LC resonator," *J. Appl. Phys.*, vol. 115, 2014, Art. no. 064508.
[46] T. S. Tuan, V. D. Lam, and N. T. Q. Hoa, "Simple design of a copolarization wideband Metamaterial Absorber for C-band applications," *J. Electron. Mater.*, vol. 48, pp. 5018–5027, 2019.
[47] S. Song, F. Sun, Q. Chen, and Z. Zhang, "Narrow-linewidth and high-transmission terahertz bandpass filtering by metallic gratings," *IEEE Trans. Terahertz Sci. Technol.*, vol. 5, no. 1, pp. 131–136, Jan. 2015.
[48] Y. Sun, H. Chen, X. Li, and Z. Hong, "Electromagnetically induced transparency in planar metamaterials based on guided mode resonance," *Opt. Commun.*, vol. 392, pp. 142–146, 2017.
[49] H. Chen, J. Liu, and Z. Hong, "Guided mode resonance with extremely high q-factors in terahertz metamaterials," *Opt. Commun.*, vol. 383, pp. 508–512, 2017.
[50] Z. Yu, H. Che, J. Liu, X. Jing, X. Li, and Z. Hong, "Guided mode resonance in planar metamaterials consisting of two ring resonators with different sizes," *Chin. Phys. B*, vol. 26, 2017, Art. no. 077804.
[51] D. H. Luu, B. S. Tung, B. X. Khuyen, L. D. Tuyen, and V. D. Lam, "Multi-band absorption induced by near-field coupling and defects in metamaterial," *Optik*, vol. 156, pp. 811–816, 2018.
[52] T. T. Nguyen and S. Lim, "Wide incidence angle-insensitive metamaterial absorber for both TE and TM polarization using eight-circular-sector," *Sci. Rep.*, vol. 7, pp. 3204, 2017.
[53] N. T. Q. Hoa, P. D. Tung, N. D. Dung, H. Nguyen, and T. S. Tuan, "Numerical study of a wide incident angle- and polarisation-insensitive microwave metamaterial absorber based on a symmetric flower structure," *AIP Adv.*, vol. 9, 2019, Art. no. 065318.
[54] H. Zhang, M. Luo, Y. Zhou, Y. Ji, and L. Chen, "Ultra-broadband, polarization-independent, wide-angle near-perfect absorber incorporating a one-dimensional meta-surface with refractory materials from UV to the near-infrared region," *Opt. Mater. Exp.*, vol. 10, pp. 484–491, 2020.
[55] M. Yoo and S. Lim, "Polarization-independent and ultrawideband metamaterial absorber using a hexagonal artificial impedance surface and a resistor-capacitor layer," *IEEE Trans. Antennas Propag.*, vol. 62, no. 5, pp. 2652–2658, May 2014.
[56] S. Ghosh, S. Bhattacharyya, and K. V. Srivastava, "Design, characterisation and fabrication of a broadband polarisation-insensitive multilayer circuit analogue absorber," *IET Microw. Antenna Propag.*, vol. 10, no. 8, pp. 850–855, 2016.
[57] H. Chen *et al.*, "Flexible and conformable broadband metamaterial absorber with wide-angle and polarization stability for radar application," *Mater. Res. Exp.*, vol. 5, 2018, Art. no. 015804.
[58] S. Kalraiya, R. K. Chaudhary, and M. A. Abdalla, "Design and analysis of polarization independent conformal wideband metamaterial absorber using resistor loaded sector shaped resonators," *J. Appl. Phys.,* vol. 125, 2019, Art. no. 134904.
[59] T. T. Nguyen and S. Lim, "Design of metamaterial absorber using eight-resistive-arm cell for simultaneous broadband and wide-incidence-angle absorption," *Sci. Rep.*, vol. 8, 2018, Art. no. 6633.
[60] J. Yang and Z. X. Shen, "A thin and broadband absorber using double-square loops," *IEEE Antennas Wireless Propag. Lett.*, vol. 6, pp. 388–391, Dec. 2007.
[61] T. T. Nguyen and S. Lim, "Angle- and polarization-insensitive broadband metamaterial absorber using resistive fan-shaped resonators," *Appl. Phys. Lett.*, vol. 112, 2018, Art. no. 021605.